SCIENCE CHINA
Information Sciences

• LETTER •

December 2025, Vol. 68, Iss. 12, 220308:1–220308:2
https://doi.org/10.1007/s11432-025-4677-3

Special Topic: Terahertz Communications for 6G and Beyond: How Far Are We?

Nonlinear behaviors of transceivers for terahertz communications: data sets and models

Kai YING[1], Weiming ZHANG[1], Pengxuan GAO[1], Linshan ZHAO[2], Yinjun LIU[3], Boyu DONG[3] & Junwen ZHANG[3*]

[1]*School of Computer Science, Shanghai Jiao Tong University, Shanghai 200240, China*
[2]*Shanghai Advanced Research Institute, Chinese Academy of Sciences, Shanghai 201210, China*
[3]*College of Future Information Technology, Fudan University, Shanghai 200433, China*

Received 8 May 2025/Revised 24 August 2025/Accepted 10 November 2025/Published online 19 November 2025

Citation Ying K, Zhang W M, Gao P X, et al. Nonlinear behaviors of transceivers for terahertz communications: data sets and models. Sci China Inf Sci, 2025, 68(12): 220308, https://doi.org/10.1007/s11432-025-4677-3

Terahertz (THz) radiation, spanning 100 GHz to 30 THz between infrared and microwave bands, offers ultra-wide bandwidths enabling terabit-per-second data rates to meet future communication demands. However, power amplifiers (PAs) in THz front-ends exhibit strong nonlinearities and significant memory effects caused by device physics and ultra-wideband challenges. These impairments degrade signal fidelity and spectral containment, limiting system performance. Conventional polynomial-based models face issues such as multicollinearity and ill-conditioning, reducing their effectiveness in modern wideband, high-frequency scenarios.

Recent advances have focused on artificial intelligence techniques leveraging neural networks nonlinear mapping capabilities. Early work by Rawat et al. [1] modeled the nonlinear behaviors of wireless power amplifiers using a dynamic real-valued time-delay structure. Subsequent models [2, 3] include convolutional neural networks and hybrid CNN-LSTM architectures, improving efficiency and accuracy. Transformer-based models [4, 5] have also demonstrated strong performance by effectively capturing long-range dependencies in PA nonlinearities.

Existing experimental validations mostly use datasets with bandwidths below 200 MHz and focus on sub-6 GHz bands. This narrow scope overlooks challenges in ultra-wideband Terahertz systems, which exhibit stronger nonlinearities and more significant memory effects. Moreover, many existing nonlinear models target narrowband or sub-6 GHz systems and often fail to generalize to ultra-wideband Terahertz scenarios. Since nonlinear behaviors vary with carrier frequency and bandwidth, a generalized modeling framework adaptable to diverse bands and conditions is essential.

To address this gap, we built a comprehensive experimental testbed covering W-, D-, and G-bands with bandwidths from 1 to 4 GHz. To the best of our knowledge, it is the first publicly available dataset for nonlinear modeling of THz transceivers. Leveraging this dataset, we propose a convolution-enhanced Transformer architecture. Our approach effectively captures complex nonlinearities and memory effects across diverse conditions. Additionally, we introduce a parameter modulation mechanism that adapts model parameters to varying domain characteristics, improving robustness and generalization across different frequency bands and bandwidths.

Dataset. We develop a THz transceiver test bed and collect input-output signal pairs across multiple frequency bands and bandwidth settings. The dataset spans W (96 GHz), D (141 GHz), and G (228 GHz) carrier frequency bands, with instantaneous bandwidths up to 4 GHz, and captures nonlinear behaviors under various modulation formats and operating conditions. It serves as the first public resource for studying ultra-wideband THz nonlinearities. Our dataset is already publicly available at the website[1)].

The THz transceiver test bed consists of an arbitrary waveform generator (Keysight M8195A, 60 GHz sampling rate), frequency mixer, the device-under-test PA (W-band: 35 dB gain AT-LNA-3504HP PA, D-band: 18 dB gain AT-PA-1815E PA, G-band: 16 dB gain AT-PA-1610 PA), 25-dBi gain transmitter/receiver horn antennas, and an oscilloscope (Agilent DSOX93204A). The oscilloscope offers high measurement accuracy with a 33 GHz analog bandwidth, 2.10 mV noise floor (at 50 mV/div, 33 GHz), and 100 fs jitter floor. The baseband signals are 16/64-quadrature amplitude modulation orthogonal frequency division multiplexing (OFDM) signals.

Baseband input signals are first digitally up-converted to an intermediate frequency (IF). Then the AWG loads IF signals to the target radio frequency (RF) bands by the mixer. The resulting RF signal is amplified by the PA and transmitted over a 1.0-meter distance via a transmitter horn antenna with 25-dBi gain. At the receiver side, a 25-dBi gain receiver horn antenna captures the signal. Finally, the RF signal is down converted to the same IF band using a shared local oscillator (LO), and then the signal is collected through

* Corresponding author (email: junwenzhang@fudan.edu.cn)

1) https://github.com/DSLabDataCenter/THz-NL.

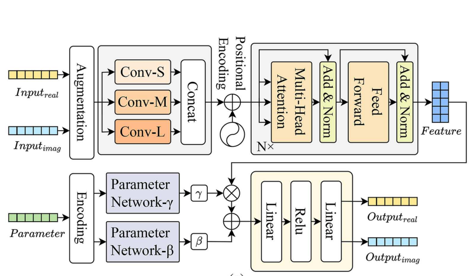

(a)

Mode	Model	All	W	D	G
None	RVTDNN	-6.38	-10.28	-10.92	-10.25
	RVRTCNN	-6.398	-10.19	-10.84	-10.20
	RVTDCNN	-6.35	-10.12	-10.81	-10.14
	ARVTDform	-7.65	-11.41	-12.28	-11.35
	ATLSTM	-6.52	-10.23	-10.89	-10.21
	ARVMCTN	**-10.83**	**-13.35**	**-14.38**	**-13.02**
Param	RVTDNN	-20.39	-19.06	-23.62	-15.58
	RVRTCNN	-20.51	-19.10	-23.64	-15.66
	RVTDCNN	-20.41	-18.99	-23.57	-15.62
	ARVTDform	-20.60	-19.13	-23.76	-16.01
	ATLSTM	-20.43	-19.12	-23.53	-15.68
	ARVMCTN	**-20.94**	**-19.51**	**-24.30**	**-17.50**

(b)

Figure 1 (Color online) (a) Model architecture diagram; (b) NMSE results (dB) of different models on datasets with various bandwidths. The best results are in bold.

an oscilloscope. The captured IF signal is processed offline (e.g., digital down-conversion) to obtain the corresponding baseband signal.

Using the above testing platform, we collect datasets of 16-QAM and 64-QAM OFDM signals at bandwidths of 1, 2, and 4 GHz in the W, D, and G frequency bands, respectively. Each frequency band contains approximately 83000 data samples, resulting in a total dataset size of about 250000 samples. Among the five independently collected datasets, four are used for training and one for testing.

Proposed method. We propose an augmented real-valued multi-scale convolutional transformer network (ARVMCTN) to model nonlinear behaviors of THz transceivers, and the model architecture is shown in Figure 1(a). The architecture captures temporal variations and long-range dependencies in complex baseband signals, while generalizing across frequency bands and bandwidths.

Each input is a temporal window of measured baseband signals, represented in an augmented real-valued form by concatenating real and imaginary parts, amplitude, and higher-order nonlinear terms.

The network uses a two-stage feature extractor. First, a multi-scale convolutional module with three parallel 2D convolution branches of different kernel sizes extracts information at multiple receptive fields. Second, these features are combined with positional encodings and passed through stacked multi-head self-attention Transformer encoder layers. The contextual features output by the Transformer encoder are fed to a fully connected regression layer that predicts the real and imaginary parts of the signal.

To address domain shifts, a lightweight parameter modulation mechanism is employed. The domain parameters from the dataset, including frequency band, carrier frequency, and bandwidth, are one-hot encoded and then passed through two small multilayer perceptrons. These generate per-feature scaling (γ) and shifting (β) factors used to modulate the intermediate features. Given intermediate feature F, modulation is $F_{\rm mod} = \gamma \odot F + \beta$, where $\odot$ is element-wise multiplication. This adapts feature distributions per domain without retraining.

Experimental setup and results. We evaluate ARVMCTN and several baselines under four training settings: joint training on all domains (All) and separate training on W-, D-, and G-band subsets, both with and without parameter modulation. RVTDNN [1] employs a dynamic real-valued time-delay structure to model nonlinear behaviors. RVTDCNN [2] further incorporates convolutional layers to better extract local temporal features. RVRTCNN [3] combines dilated convolution and residual connections, which strengthens temporal modeling ability. ARVTDform [4] integrates Transformer-based attention into the augmented time-delay framework. ATLSTM [5] adds an attention layer before the LSTM to enhance the capability of integrating information. In our experiments, the memory depth of all models is set to 10. Under this configuration, the attention-based models (ARVMCTN, ARVTDform, ATLSTM) require about 7M FLOPs with an average inference latency of 1.5 ms, while the other models remain around 4M FLOPs with 0.5 ms latency. All models exhibit a similar memory footprint of approximately 10 MB. The experiments are conducted on a platform equipped with an NVIDIA RTX 4090 GPU and an AMD EPYC 7T83 CPU.

As shown in Figure 1(b), ARVMCTN consistently outperforms all baselines, demonstrating the effectiveness of the proposed architecture. Without parameter modulation, joint training across domains leads to clear performance drops, while applying modulation yields substantial and consistent gains. Moreover, ARVMCTN surpasses the Transformer-only ARVTDform, validating the benefit of multi-scale convolutional integration.

Conclusion. We present the first large-scale THz nonlinear dataset across multiple frequency bands and bandwidths, and a convolution-enhanced Transformer architecture with parameter modulation for ultra-wideband behavioral modeling. The proposed approach effectively captures both local and long-range dependencies by employing multi-scale convolutions for different nonlinear sources and a Transformer regressor for long-range coupling effects, adapts to diverse acquisition domains. This work provides a practical modeling framework for future THz system design and DPD development.

Acknowledgements This work was supported by National Natural Science Foundation of China (Grant No. 62235005).

References

1 Rawat M, Rawat K, Ghannouchi F M. Adaptive digital predistortion of wireless power amplifiers/transmitters using dynamic real-valued focused time-delay line neural networks. IEEE Trans Microwave Theor Techn, 2010, 58: 95–104

2 Hu X, Liu Z, Yu X, et al. Convolutional neural network for behavioral modeling and predistortion of wideband power amplifiers. IEEE Trans Neural Netw Learn Syst, 2022, 33: 3923–3937

3 Yang J, Zhao W, Li Y, et al. Digital predistortion of quadrature digital power amplifiers using RVRTCNN: real-valued residual temporal convolutional neural network. IEEE Commun Lett, 2025, 29: 2028–2032

4 Zhao G, Ying K, Wen Q, et al. Analysis and behavioral modeling using augmented transformer for satellite communication power amplifiers. IEEE Internet Things J, 2025, 12: 11994–12007

5 Yang J, Zhao W, Li Y, et al. Digital predistortion for quadrature digital power amplifiers using deep neural network of AT_LSTM: attention LSTM. In: Proceedings of the Great Lakes Symposium on VLSI, New York, 2025. 784–790